Received: 9 September 2019 | Revised: 25 October 2019 | Accepted: 17 November 2019

DOI: 10.1111/jace.16923

Journal of the American Ceramic Society

ORIGINAL ARTICLE

Molecular mechanism of the expansion of silica glass upon exposure to moisture

Stephen H. Garofalini | **Jesse Lentz** | **Matthew Homann**

Interfacial Molecular Science Laboratory, Department of Materials Science and Engineering, Rutgers University, Piscataway, NJ, USA

Correspondence
Stephen H. Garofalini, Interfacial Molecular Science Laboratory, Department of Materials Science and Engineering, Rutgers University, 607 Taylor Rd., Piscataway, NJ 08855, USA.
Email: shg@glass.rutgers.edu

Funding information
National Science Foundation, Grant/Award Number: 1609044

Abstract

Molecular dynamics simulations show that the expansion of silica glass occurs by the presence of the hydroxyl (SiOH) groups present in the glass as opposed to intact water (H_2O) molecules, providing an accurate molecular description of the experimentally observed volume changes in silica glass exposed to water. Using a robust and accurate reactive potential, the simulations show that the expansion is caused by the rupture of siloxane (Si–O–Si) linkages in the glass via reactions with water molecules, forming SiOHs. Such reactions remove smaller rings and form larger rings, with a decrease in the overall number of rings smaller than a prescribed large ring size in comparison to dry glasses. This change in ring structure overcomes the inherently stronger hydrogen bonding in the glasses containing SiOH in comparison to the glasses containing predominantly intact H_2O molecules. This stronger H-bonding of the SiOH also causes a shift to lower frequencies in the high-frequency OH vibrational spectrum for the silanols, as shown in previous ab-initio calculations. This introduces a question about assuming the lower frequency part of the high-frequency peak is only due to intact H_2O molecules. A slight decrease in volume occurred in the glasses containing the largest concentration of intact H_2O molecules. There is no change in the ring size distribution between the H_2O glasses and dry glasses. Rather, the slight decrease in volume in the H_2O system is caused by a decrease in siloxane bond angles caused by the formation of H-bonds between the H_2O molecules and the glass O in the siloxane cages surrounding the H_2O molecules.

KEYWORDS

glass, silica, simulation

1 | INTRODUCTION

The behavior of water in contact with amorphous silica (a-silica) surfaces and penetration into the subsurface has garnered significant interest over many decades.[1–24] In general, water has been shown to weaken silica in tension via stress corrosion cracking at a stress less than the normal fracture stress. Such behavior is caused by the commonly known reaction of a water molecule rupturing the strained siloxane bonds at a crack tip via the Michalske-Freiman model, enabling propagation of the crack.[4,5] The Michalske-Freiman model assumes small two- and three-membered siloxane rings that have small siloxane (Si–O–Si) bond angles that show significantly increased bond rupture upon exposure to water.[3] However, Tomozawa attributed degradation in strength of silica to the presence of molecular water and surface structural relaxation.[25] Based on their IR data of changes in the high-frequency Si–O asymmetric

stretch peak, it was assumed that the presence of molecular water lowers the fictive temperature in the surface via a surface structural relaxation mechanism and lower fictive temperature silica has a lower strength.[25] However, strengthening of silica exposed to water while under tension has also been shown.[26–29]

Amorphous silica has been shown to increase volume when exposed to water at elevated temperatures.[30,31] In recent years, such an effect has been shown to occur at the glass surface of either fibers or disks exposed to water vapor.[26,29,32] In the fiber case, longitudinally polishing the glass fiber in half after exposure under low tensile stress to moist atmosphere at temperatures below the glass-transition temperature was observed to cause permanent bending.[29] The result was indicative of a surface expansion that was attributed to surface structural relaxation that causes a volume increase in the surface. Thin disks exposed to water vapor on one side similarly showed expansion on the exposed side, the curvature of which could be used to calculate a swelling stress.[32]

Such a volume increase at the surface caused by exposure to moisture would convert to a compressive stress in the surface of a glass sample whose surface is constrained by the bulk, thus increasing strength in a manner similar to ion-exchange strengthening of glass. Additional studies of silica fibers exposed to water vapor while under moderate tensile stress less than the fracture stress and temperatures below the glass fictive temperature also showed, upon release of the applied tension, an increase in the fracture stress.[27]

In either strength degradation or strength enhancement, one group assumes from IR data that surface structural/stress relaxation is caused by the presence of molecular water,[25,27–29,33] whereas another group concludes that expansion of silica occurs via formation of silanols (SiOHs) rather than molecular water in the glass.[26,32,34,35] The attribution of H_2O molecules as the cause of strength enhancement is based on the difference in the depth of the high-frequency IR peak of the OH moiety on Si (SiOH) vs the depth of the change in the high-frequency IR peak of the asymmetric stretch of the Si–O–Si group indicative of a relaxation process. The latter continues to a greater depth than the former and is attributed to an undetectable amount of molecular water.[28,33,36] Since the molecular water was undetectable by IR, it was assumed that such a low concentration would have to travel significant distances to affect sufficient structural relaxation over a sufficient volume of the glass to affect properties.[27,29] A proposed mechanism was the dissociation of a water molecule and proton transfer to another water to create an OH^- and H_3O^+ ion pair. The excess proton would then migrate from the H_3O^+ ion to a bridging oxygen (BO) and cause a lowering of the Si–O–Si bond angle at that oxygen.[27,29] The proton then leaves the BO, but the lower Si–O–Si angle is retained, acting as a stress reliever. That is, the change in angles affect surface stress/structural relaxation. However, molecular dynamics simulations using a highly robust and accurate multibody potential showed that protons are only very weakly bonded to the BO with bond angles near the average for siloxane bonds (145°-150°) and do not cause the angle to change by more than a degree or two.[14] Only pre-existing siloxane bond angles near the 135° range showed stable sites for proton adsorption.[14] The results of those simulations showed that a proton on a siloxane bridge matches the adsorption site preference and energy obtained in ab-initio calculations of protons on bridging oxygen.[37,38] Another proposed mechanism for strength degradation of silica exposed to atmosphere at high temperature is surface crystallization.[39]

A major question arises as to the mechanism governing the volume increase and the strengthening caused by the presence of moisture, either, as mentioned above, as molecular water or as hydroxyls (SiOH).

In order to address this question at a molecular level, molecular dynamics computer simulations using a robust, transferrable reactive interatomic potential[13,20,40] has been used to address the effect of molecular water vs hydroxyls in amorphous silica on volume in comparison to dry silica.

The simulations employ the reactive multibody potential developed in our lab that has been shown to reproduce multiple properties of bulk water and water at glass interfaces under various conditions with results consistent with a variety of experimental and ab-initio data. While designed to match the density-temperature curve for bulk water, the structure matches the experimental data by Soper.[40,41] Other accurately predicted properties include heat of vaporization (10.4 kcal/mole), diffusion coefficient (2.4×10^{-5} cm^2/s vs 2.3×10^{-5} cm^2/s), frequency spectrum, and dipole moment.[40] Subsequent application of the potential in simulations of water on the amorphous silica surface showed reactions and formation of silanols (SiOH) in concentrations consistent with experiment (4-5/nm^2). These include isolated, vicinal, geminal silanols, and a small concentration of $SiOH_2$ sites caused by short-lived non-dissociative chemisorption of a water molecule onto an exposed three-coordinated Si surface site; such $SiOH_2$ sites have been seen experimentally[42] and in DFT calculations of water on oxide surfaces.[43] The simulations also show proton transfers involving water molecules adjacent to the glass surface and surface sites, with formation of H_3O^+ ions. The lifetimes of H_3O^+ ions in bulk water are consistent with that observed experimentally and in ab-initio calculations of such species[44]; their lifetimes adjacent to the glass surface are much shorter-lived[45] and the proton transfer mechanisms are the same as those seen in ab-initio calculations.[10,13,20,43]

Simulations with this potential also showed proton transfer from an H_3O^+ ion in bulk water via formation of Eigen and Zundel complexes that resulted in the proton transferring while in the Zundel complex, with an energy barrier of 0.8 kcal/mole,[44] consistent with ab-initio calculations that showed a value of 0.6 kcal/mole[46] at the same 2.4 Å O–O spacing as the simulations.

Extending the evaluations to simulations of water nanoconfined in amorphous silica resulted in the simulations showing the change in volume with decreasing pore size seen experimentally.[12,16] Simulations of hydrogen bond lifetimes of water molecules in bulk water gave a time constant of 2.1 ps,[47] consistent with the experimental data.[48]

2 | COMPUTATIONAL PROCEDURE

The molecular dynamics (MD) simulations employed the "MG" reactive multibody potential previously presented[14,40] and discussed above. A bulk silica glass was made from a β-cristobalite crystal containing 11 664 atoms with dimensions ~64Å × 64 Å × ~43 Å and melted at 6000 K followed by cooling through intermediate temperatures to 298 K over 5.5×10^6 timesteps. The system was then remelted at 6000 K and the same cooling process occurred, except over 60.0×10^6 timesteps, all with a timestep of 1.0 fs (=60 ns). At each temperature, a constant number, volume, temperature (NVT) ensemble was used and the volume was adjusted according to the experimental thermal expansion coefficient of 5.5×10^{-7}. An additional run of 1×10^6 timesteps was used to generate the final volume for the dry glass at 1 atmosphere under the constant number, pressure, and temperature (NPT) ensemble, again with a timestep of 1.0 fs (=1 ns). These silica glasses had a density of 2.21 g/cm^3 and only 33 non-bridging oxygen (of 7776 silica oxygens). An example of the stability of the system dimensions in the final 1 ns run under the NPT ensemble and the Berendson thermostat is shown in Figure 1. The resultant glass was used to make the glasses containing either molecular water or reacted waters that form silanols. That is, all of the glasses containing H_2O molecules or predominantly hydroxyls were begun from the same dry glass.

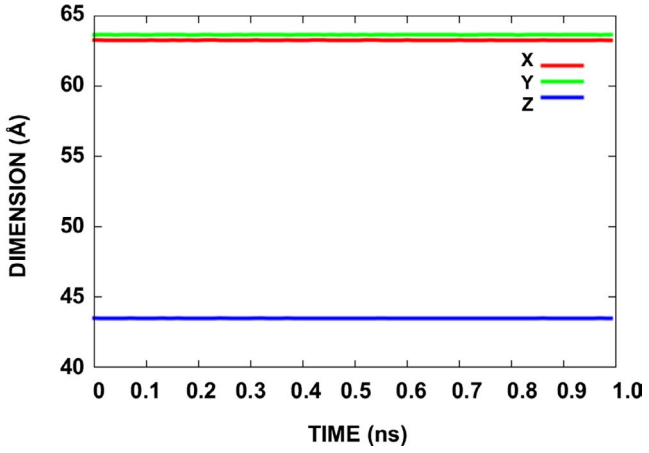

FIGURE 1 Dry glass dimensions over 1 ns NPT run at 298 K and labeled DRY in figures below [Color figure can be viewed at wileyonlinelibrary.com]

For the systems with molecular water, eight different random spatial distributions of 194 water molecules (5 mol%) were added to the starting bulk glass at room temperature and called the "initial wet" systems. The random insertion of the water molecules included a distance cut-off of the water oxygen from any other waters and any silica atoms of 2.8 Å. This insured that the inserted waters were not too close to any glass atoms that might inadvertently create an Si–Ow (water oxygen) bond or SiOH. The distance is also the same to the O–O spacing in bulk water. Each glass was run under NPT conditions for 6.5×10^6 timesteps, with a timestep of 0.1 fs for all systems containing H. These systems were labeled "wet" or "H_2O" in the text and figures below to indicate that they contain predominantly intact H_2O molecules. While data below compare these wet glasses to the dry glass run for 1×10^6 timesteps at 298K with a 1.0 fs timestep, an additional long run of 1×10^7 timesteps at 0.1 fs was used in the dry glass to determine if there were any differences with using the smaller (0.1 fs) or larger (1.0 fs) timesteps for the same total time (1 ns) in the dry glasses. The resulting volumes of the 2 dry glasses were the same within six significant figures.

For formation of the systems with reacted waters, called the "OH" or "SiOH" systems, the same eight "initial wet" systems were heated to three different elevated temperatures (1273, 1573, or 1773 K) under NVT (constant number, volume, and temperature) for 1×10^6 timesteps in order to allow for reactions to form SiOH. As stated above, the timestep was 0.1 fs for all systems containing protons. These temperatures are well below the glass-transition temperature using this potential, which is above 2225 K. The different elevated temperatures increased dissociation of the water molecules, enabling determination of the effect of different concentrations of SiOH on volume changes. The resultant OH glasses at each elevated temperature were then quenched directly to 298 K and run at 298 K for 6.5×10^6 timesteps under NPT conditions, forming eight glasses that had been heated at 1273 K quenched to 298 K, eight glasses heated to 1573 K quenched to 298 K, and eight glasses heated to 1773 K quenched to 298 K. (See Table 1.) In addition, the original dry glass was separately heated to each elevated temperature for 1.05×10^6 timesteps and quenched to 298 K and run for 2×10^6 timesteps using the 1.0 fs timestep (most comparisons below relate to the 1773-298 K glass that has the highest concentration of SiOH (labeled SiOH 7.7) and the dry glass that experienced the same heat treatment that is labeled DRY* in the figures below). A run for the dry glass at 298 K

TABLE 1 Protocol

System (Label)	Temperature (K)	Number of systems
Dry (Dry)	298	1
Wet (H_2O)	298	8
Dry	1273 → 298	1
Wet (SiOH 2.2)	1273 → 298	8
Dry	1573 → 298	1
Wet (SiOH 5.2)	1573 → 298	8
Dry (Dry*)	1773 → 298	1
Wet (SiOH 7.7)	1773 → 298	8

from the elevated temperature for 10×10^6 timesteps gave the same results as observed at 2×10^6 timesteps, indicating that the volumes reached equilibrium quickly and longer runs were unnecessary. Volumes of all glasses were calculated from an average the volumes over the 298 K runs. Therefore, there is 1 dry glass at 298 K, 1 dry glass and 8 SiOH glasses heated to 1273 K and quenched to 298 K (later labeled "SiOH 2.2" in figures based upon the concentration SiOH in the glass), 1 dry glass and 8 SiOH glasses heated to 1573 K and quenched to 298K (labeled "SiOH 5.2" below), and 1 dry glass (labeled DRY*) and 8 SiOH glasses heated to 1773 K and quenched to 298 K (labeled "SiOH 7.7" below), plus 8 "H_2O" glasses with predominantly intact H_2O molecules run only at 298 K (labeled "wet" or "H_2O" below). (See Table 1.) The volume of the H_2O glasses was averaged over the 8 H_2O systems and the volume of each SiOH glass system was averaged over the eight glasses of the specific system containing different concentrations of SiOH, enabling a view of the change in volume with changing SiOH concentration.

Volume differences between the H_2O and dry systems and each SiOH system and its concomitant dry system were calculated and the volume change vs SiOH and molecular water contents were determined. Of course, there were some silanols in the H_2O systems and some unreacted H_2O molecules in the SiOH systems and these concentrations are seen in the resultant graph shown below regarding volume changes vs concentrations.

In addition to the volume changes, pair distribution functions (PDF), ring size distributions, siloxane (Si–O–Si) bond angle distributions, vibrational spectra, and convex hull volumes around O from the water constructed from Voronoi neighbor calculations were evaluated in order to provide an atomistic understanding of the resultant volume differences between dry and wet vs dry and hydroxylated systems.

For the convex hull calculations, the O from the glass are labeled Osi and those for the water are labeled Ow. Thus there are Osi in the dry glasses and the same Osi in the wet and SiOH glasses. For each Ow, three shells of neighboring Osi were determined using the following procedure. For each saved configuration and each Ow, a subset of the system consisting of all network-forming Osi and that one single Ow atom was constructed. A Voronoi polyhedron was constructed around the Ow atom using the Voro++ library[49] and the resulting set of Voronoi neighbors for this specific Ow were labeled Osi^1, where the superscript indicates the first or 1 shell of Osi around this Ow. A second shell of Osi^2 around this Ow atom was generated and consists of all Osi atoms, excluding Osi^1, that are connected to one or more Osi^1 neighbors through a pair of O–Si bonds. Specifically, if Oa is an Osi^1 neighbor, then Ob is an Osi^2 neighbor if there exists a Si atom such that the Si–Oa and Si–Ob distances are each less than 2.1 Å. A third shell of neighbors attached to the 2nd shell Osi was similarly constructed but had a high probability of including the shells of other Ow and is not considered here. After constructing these Osi neighbor lists for each Ow, convex hull volumes were calculated using the Osi of each shell's neighbor list as vertices in both the wet (OH) systems and the corresponding dry system. Therefore, the differences in convex hull volumes in the dry vs the H_2O or OH system are specific to the same Osi per system. QHull was used to calculate the convex hull volumes.[50] The volume change of a neighbor list was calculated as $\Delta V = V_{wet} - \langle V_{dry} \rangle$ (or $\Delta V = V_{oh} - \langle V_{dry} \rangle$), where V_{wet} (V_{oh}) is the convex hull volume of the neighbor list in the relevant configuration of an H_2O or OH system and $\langle V_{dry} \rangle$ is the average of the volume of the same neighbor list of atoms of the corresponding dry system (glasses 1-8).

3 | RESULTS AND DISCUSSION

Figure 2 shows the change in volume as a function of the concentration of intact H_2O molecules (red squares labeled H_2O)

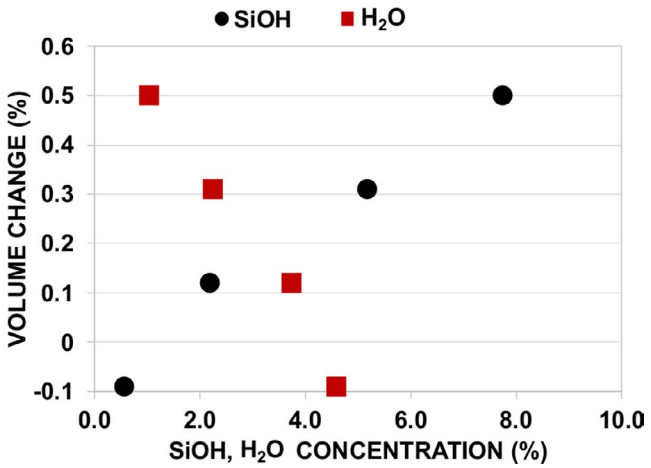

FIGURE 2 Volume changes in the bulk glasses at different concentrations of SiOH (black dots) and concurrent H_2O's (red squares) (in mol%) in the same glasses in comparison to the appropriate dry glasses [Color figure can be viewed at wileyonlinelibrary.com]

and SiOH (black circles labeled SiOH) in each set of eight glasses with these different concentrations of constituents. (A small fraction of hydroxide ions form and are uncounted here.) The glasses with the highest concentration of intact H_2O molecules (red square at ~4.6% concentration) were generated from the glass with intact H_2O molecules that only experienced the 298 K run. Since not all of the original H_2O molecules remain intact for the wet systems and not all of the water molecules dissociate to form SiOH in the OH systems, the data points are horizontally paired such that a particular volume will have a percentage of SiOH and a remaining percentage of H_2O (or visa-versa). Therefore, the coupled horizontal points show the concentration of each constituent (H_2O or SiOH) on the horizontal axis for the volume change experienced with that composition on the vertical axis. It is clear from Figure 2 that an increase in the concentration of SiOH causes an increase in the volume of the resultant glasses in comparison to the similarly processed dry glasses. That is, as mentioned above, the volumes of the glasses that experienced the higher temperature heating in order to generate increased SiOH concentrations were compared to that of the dry glasses that experienced the exact same heat treatment procedure, precluding the effect of such heat treatment affecting the volume differences shown in the figure. The results shown here are consistent with the conclusions presented by Wiederhorn et al[32] that it is the SiOH that cause the volume expansion and not the intact H_2O molecules. There is no such increased volume in the case of the glasses with molecular water. Surprisingly, there is a slight loss of volume with the H_2O systems, as discussed below.

The most obvious rationale for the cause of the increase in the volume of the glasses containing SiOH would be the rupture of siloxane (Si–O–Si) bonds in the reactions with the water molecules. Such reactions would cause an opening of the ring structure of the glass and expansion of the overall volume. Figure 3 shows an example of the change in the ring structure at the site of the reaction involving formation of an SiOH bond, rupturing an Si–O–Si bond. The dry glass structure is given by the black Si–O bonds near the reaction site while post reaction is given by the cyan Si–O bonds. Rupture of the Si–O–Si bond at the orange O, forming the SiOH (orange O with red OH bond and red proton) removes two rings (black) and creates one larger ring (cyan) and movement of the two blue Si at this original Si–O–Si site (black) to new positions upon rupture of the siloxane bond (cyan) expands the larger resultant cyan ring.

Variation in the ring structure can be verified in the simulations by looking at the change in the ring structure of the sets of systems. The distribution of shortest-path rings is shown in Figure 4A for the dry glass (no moisture added), the average in the glasses with mostly intact water molecules (H_2O) and the average in the glasses with the highest concentration of SiOH (SiOH 7.7). There is little difference between the H_2O system and the dry glass. However, for the SiOH 7.7 glasses, there is a

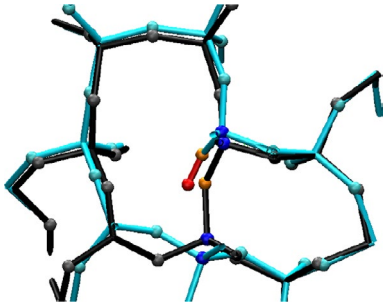

FIGURE 3 Snapshot of the effect of rupture of an Si–O–Si bond, forming an SiOH, on the original dry glass rings (black SiO bonds) to the new ring structure (cyan). Orange spheres depict the same reacting O, blue spheres are relevant Si, other spheres are O in dry (gray) and SiOH 7.7 (cyan) glasses. Red sphere is H with red SiOH bond [Color figure can be viewed at wileyonlinelibrary.com]

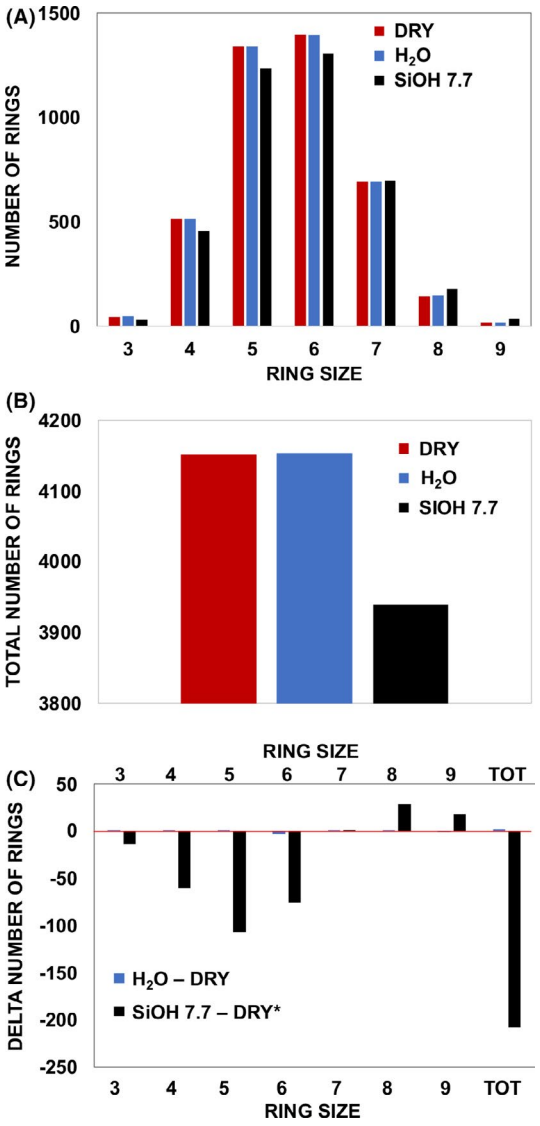

FIGURE 4 A, Ring size distribution in the three systems; B, total number of rings in each system (note y axis); C, difference in number of rings for exposed glasses vs dry (H_2O difference barely discernible) [Color figure can be viewed at wileyonlinelibrary.com]

decrease in the smaller ring sizes, with an increase in the largest rings (there are no two-membered rings in the glasses). The total number of rings for each system is shown in Figure 4B, again showing the similarity between the dry and H_2O glasses and loss in the SiOH 7.7 system (note the values on the y-axis in the inset image). Figure 4C shows the differences in the various ring sizes between the H_2O and Dry glass and the SiOH 7.7 and DRY* glass, providing a better view of the changes that occur. The difference between the H_2O system and the DRY glass is barely discernible. (Note, the DRY and DRY * gave same results.) There is a significant loss in the total number of rings in the SiOH 7.7 glasses in comparison to the relevant dry glass.

Such results are consistent with the expansion of the glasses that had the reactions with the water molecules to form the SiOH. However, what is the cause of the slight contraction of the glasses that had the highest concentration of intact water molecules and fewest SiOH, as shown in Figure 2?

Evaluation of the local structure of the glasses can provide a useful answer. The differences between the siloxane (Si–O–Si) bond angle distribution for the H_2O and SiOH 7.7 and their respective dry glasses are shown in Figure 5, grouped in small (116°-135°), medium (136°-155°), and large (156°-175°) angles. It is clear that there is a significant loss of the small angles in the SiOH 7.7 system, consistent with the expected water molecule reactions and rupture of small (strained) siloxane bonds. Interestingly, there is a larger increase in the small angle siloxane bonds for the H_2O system in comparison to the medium and large bond angles. Since there is no change in the number of rings in the H_2O system in comparison to its dry glass, this increase in the small bond angles is indicative of a relaxation and bending of the siloxane bonds near the H_2O molecule caused by the H-bonds between the H_2O molecule and the O in the siloxane bond. This increase in smaller angles would be a contributor to the decreased volume of the H_2O glasses in comparison to the dry glass, as shown next.

Figure 6 shows six images as a function of time of a water molecule within a cage of siloxane bonds (cyan) in the glass that provide a graphic indication of the formation

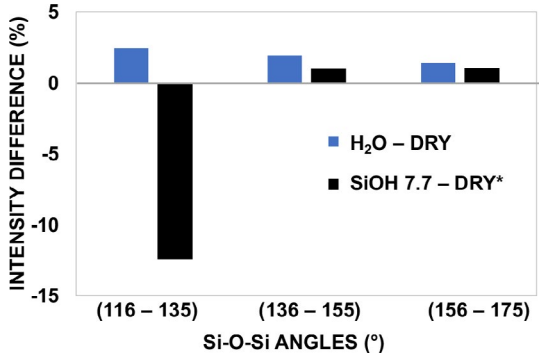

FIGURE 5 Siloxane bond angle changes between the H_2O and SiOH 7.7 systems and their appropriate dry glasses [Color figure can be viewed at wileyonlinelibrary.com]

of H-bonds between the molecule and the glass oxygens. The red lines indicate H-bonds between the protons and the O in the glass. The double H–bond formation dominates in the simulations, but configurations such as in (A) and (F) also occur, with probalities (B-E)»(F)>(A). In all times of this molecule in this cage, the H–O–H bond angle in the water only varied between 103° to 111°, with the lower numbers for the isolated molecule (A), and the higher values for the doubly H-bonded configurations. Each H-bond causes a slight lowering of the siloxane bond angle for the time of the bond and the overall effect is to create a slight decrease in volume.

The pair distribution functions (PDFs) centered on O originally from water (Ow) out to all other O in the systems are shown in Figure 7 and labeled "Ow-O," as well as the PDFs centered on all O to all other O and labeled "all O-O." First, the all O-O PDFs in the dry glasses (reddish lines) are equivalent to each other and not distinguishable in the image. Similarly, the all O–O of the H_2O and SiOH 7.7 systems glasses (greenish lines) are similar to the all O–O for the dry glasses except for a slight decrease in the height in the first O–O PDF in the H_2O system and a slight increase in the minimum near 3.1 Å for both the H_2O and SiOH systems. These slight differences can be explained by the Ow-O PDFs for those two systems also shown in Figure 7.

The first Ow-O peak in the SiOH system is indicative of those Ow from the water that attached to the Si, forming the SiOH that interact with the O near-neighbors on that Si atom and are at a distance that is consistent with the O–O spacing in silica (~2.6 Å). The H_2O system shows only a shoulder at that distance in its Ow–O PDF since few SiOH exist in the H_2O system. This causes the slight decrease in the first peak in the all O–O PDF for the H_2O system. The first large Ow–O peak in the H_2O system is at a distance near 3.1 Å and is indicative of the presence of the intact water molecules in siloxane "cages." It is also close to the O–O distance between water molecules in bulk water (2.8 Å), although the width of this peak in Figure 7 is wider on the longer distance side. The SiOH system shown in Figure 7 also has a smaller peak at ~3.1 Å, the same location as the first large peak in the H_2O system, caused by the remnant intact water molecules in the SiOH system. These peaks at ~3.1 Å cause the slight increase in the all O–O PDFs for the H_2O and SiOH systems at this distance in those PDFs.

Pair distribution functions of the HO distances for the four sets of glasses are shown in Figure 8. The first peak, indicative of the covalent OH bond, is shown in Figure 8A, showing an elongation of the covalent OH bond length for those glasses containing increasing concentrations of SiOH. Previous studies show that an increase in longer distance covalent OH bonds occurs simultaneously with a decrease in the hydrogen bond (H-bond) length.[47] Figure 8B shows the PDFs at longer distances for each system. Consistent with the elongation of the

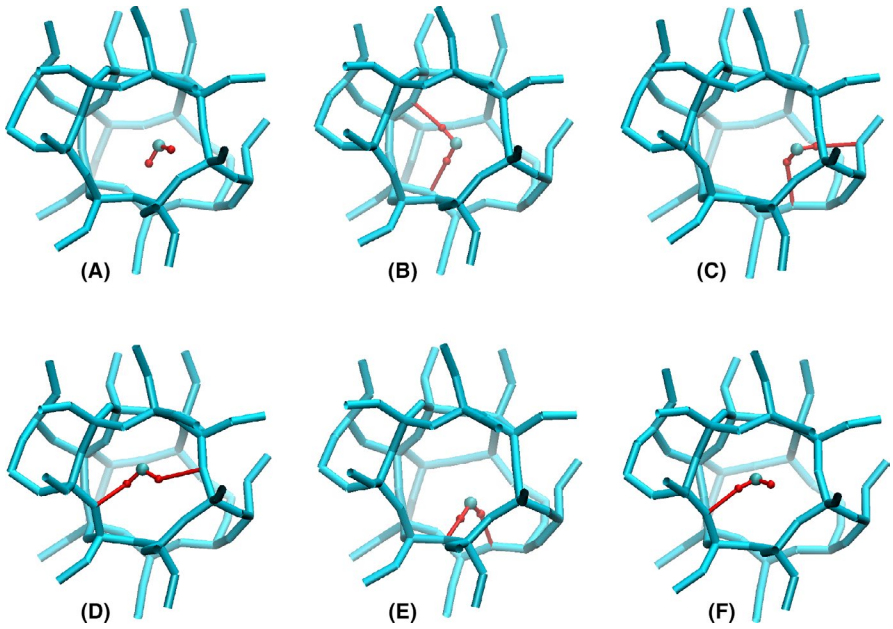

FIGURE 6 Images of a water molecule in the cage structure of the silica glass at different times showing in (A) no H-bonds and (B-E) double H-bonds and (F) a single H-bond to the cage oxygen. H-bonds shown in red [Color figure can be viewed at wileyonlinelibrary.com]

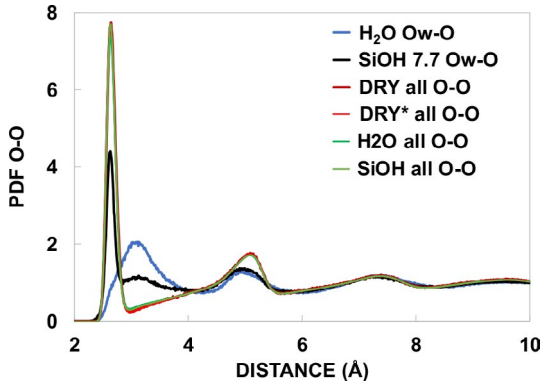

FIGURE 7 Comparison of O-O PDF's centered on the Ow in the H_2O and SiOH systems and the all O–O PDF's for the dry glasses and the H_2O and SiOH 7.7 systems [Color figure can be viewed at wileyonlinelibrary.com]

covalent bonds is the decrease in the H-bond length, as shown in the first peak in Figure 8B (such results will be relevant to the results regarding the vibrational spectra presented below). In addition, the OH pair distance curves shown in 8b are shifted to shorter distance for the SiOH systems vs the wet systems. With an increase in the number of reacting waters, forming increasing concentrations of SiOH, there is a decrease in the H-bond distance shown in the first peak of Figure 8B.

This elongation of the covalent OH bond with increasing SiOH in the glass caused by stronger H-bonding with O neighbors (shown by the decrease in the first peak in Figure 8B) is known to cause a lower vibrational frequency in the high-frequency peak of the OH spectrum.[51] Such an effect has been used in femtosecond pump-probe spectroscopies to determine lifetimes of H-bonds in water and reorientation times.[51–55] Molecular dynamics simulations using the potential used in the current work similarly showed the dependence of the shortening of the H-bond length on the elongation of the covalent OH bond length and the decrease in the high-frequency OH stretch vibration.[47]

Figure 9 shows the high-frequency OH stretching mode of the H_2O and SiOH 7.7 systems performed at 80 K. Clearly, there is an increase at the lower end of the vibrational spectrum in the glasses containing the high concentration of SiOH, consistent with the shortening of the H-bond length and concomitant increase in the covalent OH bond length and weakening of the covalent OH bond. Such results are also consistent with the data by Sulpizi et al regarding the vibrational spectra of silanols[56] as well as further discussions regarding internal silanols.[57] The assumption that the lower frequencies in the OH stretching mode observed experimentally are only due to bound H_2O molecules would be incorrect.

Consistent with volume changes seen in Figure 2 are the convex hull calculations that provide the volume of first shell or second shell O neighbors around a site. The difference between the convex hull volume of the first and second shells of bridging oxygens surrounding each Ow from each of the H_2O glasses and the volume of the exact same oxygens in the dry glass was calculated; similarly, the same difference calculation for the convex hull volumes of bridging oxygens around the added Ow in the SiOH 7.7 systems and the same relevant oxygens in the dry glass that followed the same heat-quench cycle (1773 to 298 K) was calculated. Results are shown numerically in Table 2. The overall bulk volume decrease and increase in the H_2O vs the SiOH 7.7 glasses, respectively, are shown in the second column. With an increase in the number of reacting waters, forming increasing concentrations of SiOH, there is a

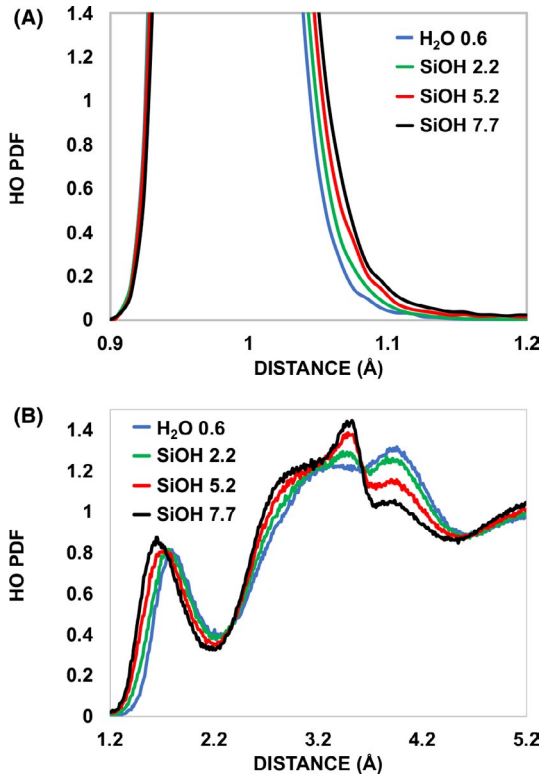

FIGURE 8 A, First peak in the HO PDF, indicative of the covalent HO bond, averaged over the 8 glasses in each system; B, Longer range HO PDF for the glasses showing the shorter HO distance for the SiOH glasses in comparison to the H_2O glasses. The numbers in the labels are the concentration of SiOH's in each system, in which the H_2O system has a minor concentration of SiOH's [Color figure can be viewed at wileyonlinelibrary.com]

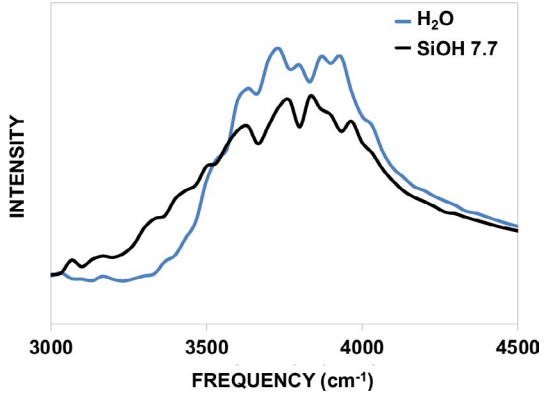

FIGURE 9 OH vibrational spectrum for the H_2O and SiOH 7.7 systems at 80 K [Color figure can be viewed at wileyonlinelibrary.com]

decrease in the H-bond distance shown in the first peak of Figure 8B. Such results are consistent with the greater decrease in the convex hull first shell volumes in the SiOH 7.7 vs the H_2O glasses (-1.93×10^{-22} vs -1.31×10^{-22} cm^3, respectively). For the H_2O and SiOH 7.7 glasses, the convex hull first shells show a slight shrinkage in comparison to the relevant dry glasses whereas the second shell shows an expansion for the SiOH 7.7 system. This expansion in second shell volumes is a significant fraction of the overall bulk expansion of the SiOH 7.7 glasses. This local volume increase in the second shell of bridging O surrounding the Ow that have formed predominantly SiOH is indicative of the rupturing of the original siloxane bonds at the sites where silanols form.

As a final test of the behavior of these systems, the H_2O glasses (that showed a slight contraction in volume with respect to the dry glass) and the SiOH 7.7 system (that showed the highest expansion with respect to its similarly processed dry glass) were all rerun in simulations in which the presence of all H and Ow were excluded. That is, the force calculations were run over only the Si and Osi in the glasses and the H and Ow were not present in the calculations. The runs were at 298 K for 150 ps under NPT conditions. The resulting volumes were calculated and compared to the original dry glasses and the results are shown in Figure 10. The original SiOH 7.7 and H_2O volume changes are shown as the black circle and red square, respectively, similar to Figure 2. Recalculating the volume of each of these systems without inclusion of the H and Ow in the calculations resulted in a decrease in the volume of the SiOH system and increase in the H_2O system to the same volumes as the original dry glasses appropriate to the system. This provides additional evidence that the H_2O molecules cause the contraction of the glasses in that system of glasses. That is, without the presence of the intact H_2O molecules in the glasses during the calculations, there is a loss of the H-bonding that is depicted in Figure 6, causing the silica to relax back to its original dry glass volume. Oppositely, the SiOH 7.7 glasses showed siloxane bond reformation when the influence of the Ow and H were removed from the calculations, causing the silica to relax back to the volume of the dry glass similarly processed (dry*), as shown next.

Since the SiOH glasses showed rupture of siloxane bonds and significant reduction in the ring size distribution in comparison to the dry glass shown in Figure 4, evaluation of the ring size distribution in the SiOH 7.7 system after relaxation without inclusion of the H and Ow in the glasses resulted in a significant return to a distribution similar to the original dry glass, as shown in Figure 11. (Note that since there was no change in the ring size distribution in the H_2O system, no additional calculations were needed.) Clearly, without the presence of the Ow and H ions, the glasses returned to the same ring size distribution as the dry glass, indicating a significant recovery of the ruptured siloxane bonds with exclusion of the H and Ow from the additional calculations.

Thus the reduction in volume of the SiOH 7.7 system upon exclusion of H and Ow to the dry glass volume and the recovery of the ring size distribution to that of the dry

TABLE 2 Convex hull volumes around 1st and 2nd shell oxygens in comparison to overall volume differences in the systems with respect to the dry glasses

System	Overall system volume difference (cm^3)	Convex hull volume differences (cm^3)	
		1st shell	2nd shell
H_2O-Dry	-1.5×10^{-22}	-1.31×10^{-22}	-1.91×10^{-22}
SiOH 7.7-Dry*	$+8.75 \times 10^{-22}$	-1.93×10^{-22}	$+7.27 \times 10^{-22}$

Note: Dry* indicates dry glass that followed the 1773K to 298K protocol that was used in the SiOH 7.7 glasses.

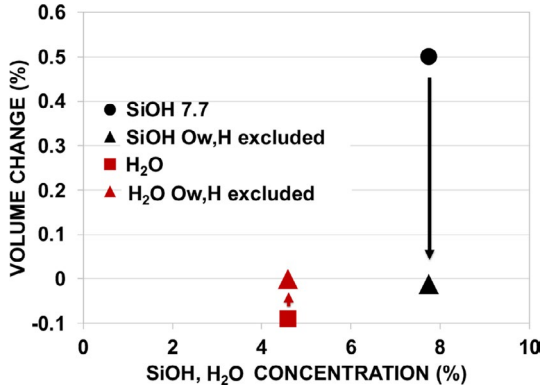

FIGURE 10 Comparison of volume change between the glasses exposed to moisture and their appropriate dry glasses in SiOH 7.7 and the H_2O systems (square and circle from Figure 2) and the change in volume of these same glasses with their dry glasses but with Ow and H excluded from the calculations of the SiOH and H_2O glasses. Each system shows relaxation back to its dry glass volume [Color figure can be viewed at wileyonlinelibrary.com]

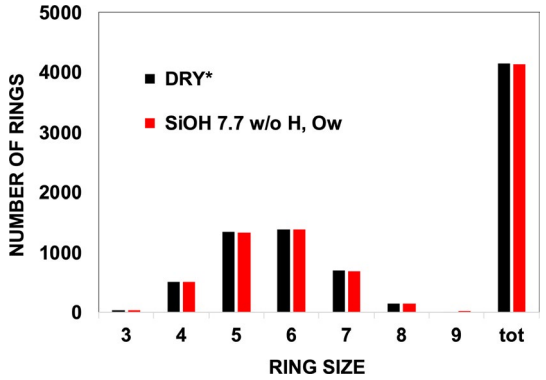

FIGURE 11 Ring size distribution of the original dry glass (DRY*) and the SiOH 7.7 glass relaxed without including H and Ow in the force calculations. A significant recovery of the ring distribution similar to the dry glass occurs [Color figure can be viewed at wileyonlinelibrary.com]

glass provide additional confirmation of the role of the formation of the silanols and ruptured rings on the expansion of the glasses containing SiOH. This is also consistent with the volume differences for the second shell data from the convex hull calculation shown in Table 2, where the second shell volume difference between the SiOH 7.7 glass and its dry glass is close to that of the overall volume difference of the SiOH 7.7 system and its dry glass. The volume increase is near the reacting sites and the additional simulations without including the H and Ow present in the SiOH 7.7 glass in the calculations allowed for a repolymerization of most of these ruptured bonds, enabling relaxation to the original dry glass structure and volume.

4 | CONCLUSIONS

Using a robust, accurate, and transferrable reactive interatomic potential, the molecular dynamics simulations show that the expansion of silica glass occurs by the presence of the hydroxyl (SiOH) groups in the glass as opposed to intact water (H_2O) molecules. The expansion is caused by the rupture of siloxane (Si–O–Si) linkages in the glass, forming SiOH, removing smaller rings and forming larger rings, with a decrease in the overall number of rings in comparison to dry glasses. This expansion is also seen in the increase in the second shell volumes surrounding the O at the SiOH sites in the convex hull calculations. This change in ring structure overcomes the inherently stronger hydrogen bonding in the glasses containing mostly SiOH in comparison to the glasses containing mostly H_2O molecules. Importantly, this stronger H-bonding in the SiOH glasses is reflected in the high-frequency OH stretch vibrational spectrum, creating an increase in the low-frequency side of this peak that overlaps the region associated with H-bonding involving H_2O molecules. This result can lead to an incorrect assumption regarding the presence of intact water molecules in the glass structure.

A surprising slight decrease in volume occurred in the glasses containing predominantly intact H_2O molecules. This is also reflected in the decrease in the convex hull volumes calculated out to both first and second neighbor shells for the glasses containing predominantly intact H_2O molecules. This decrease is caused by the formation of H-bonds between the H_2O molecules and the neighbor oxygens in the siloxane cage structure in the glass. This H-bonding is also reflected in the increase in the number of smaller siloxane bond angles in H_2O system with respect to the dry glass, even though there is not a change between the

number of small rings in the H_2O system and the dry glass. The O in the H_2O molecules (labeled Ow) form a peak in the PDF between these Ow and O in the silica structure at a distance (~3.1 Å) that is shorter than the common distance between O in different silicon tetrahedra (~5 Å). The presence of the intact H_2O molecules within the cages creates shorter Ow-O spacings that enable H-bonds between the water molecule and the O in its surrounding siloxane cage that provide an attractive force that creates a slightly smaller cage structure. The sum of all these slightly smaller cages reduces the overall volume of the glasses containing predominantly H_2O molecules.

ACKNOWLEDGMENTS

The authors acknowledge support from National Science Foundation Enviromental Chemical Science Program of the Division of Chemistry, grant number 1609044.

ORCID

Stephen H. Garofalini https://orcid.org/0000-0003-1718-2034

REFERENCES

1. Michel D, Kazansky VB, Andreev VM. Study of the interaction between surface hydroxyls and adsorbed water molecules on porous glasses by means of infrared spectroscopy. Surf Sci. 1978;72:342–56.
2. Sauer J, Schroder KP. Geminal hydroxyls on silica surfaces and their role in water adsorption. Z Phys Chemie Leipzig. 1985;266(2):379–87.
3. Bunker BC, Haaland DM, Michalske TA, Smith WL. Kinetics of dissociative chemisorption on strained edge-shared surface defects on dehydroxylated silica. Surf Sci. 1989;222:95–118.
4. Michalske T, Freiman S. A molecular interpretation of stress corrosion in silica. Nature. 1982;295(5849):511–2.
5. Michalske TA, Bunker BC. Slow fracture model based on strained silicate structures. J Appl Phys. 1984;56(10):2686–93.
6. Brinker CJ, Brow RK, Tallant DR, Kirkpatrick RJ. Surface structure and chemistry of high surface area silica gels. J Non-Cryst Solids. 1990;120:26–33.
7. Feuston BP, Garofalini SH. Water-induced relaxation of the vitreous silica surface. J Appl Phys. 1990;68:4830–6.
8. Xiao Y, Lasaga AC. Ab initio quantum mechanical studies of the kinetics and mechanisms of silicate dissolution: H+(H_3O+) catalysis. Geochim Cosmochim Acta. 1994;58:5379–400.
9. Pelmenschikov A, Strandh H, Pettersson LGM, Leszczynski J. Lattice resistance to hydrolysis of Si-O-Si bonds of silicate minerals: ab initio calculations of a single water attack onto the (001) and (111) beta-cristobalite surfaces. J Phys Chem B. 2000;104:5779–83.
10. Ma Y, Foster AS, Nieminen RM. Reactions and clustering of water with silica surface. J Chem Phys. 2005;122:144709.
11. Du JC, Cormack AN. Molecular dynamics simulation of the structure, hydroxylation of silica glass surfaces. J Am Ceram Soc. 2005;88:2532–9.
12. Garofalini SH, Mahadevan TS, Xu S, Scherer GW. Molecular mechanisms causing anomalously high thermal expansion of nanoconfined water. Chem Phys Chem. 2008;9:1997–2001.
13. Mahadevan TS, Garofalini SH. Dissociative chemisorption of water onto silica surfaces and formation of hydronium ions. J Phys Chem C. 2008;112:1507–15.
14. Lockwood GK, Garofalini SH. Bridging oxygen as a site for proton adsorption on the vitreous silica surface. J Chem Phys. 2009;131:074703.
15. Xu S, Simmons GC, Mahadevan TS, Scherer GW, Garofalini SH, Pacheco C. Transport of water in small pores. Langmuir. 2009;25:5084–90.
16. Xu S, Scherer GW, Mahadevan TS, Garofalini SH. Thermal expansion of confined water. Langmuir. 2009;25:5076–83.
17. Murray DK. Differentiating and characterizing geminal silanols in silicas by 29Si NMR spectroscopy. J Coll Interface Sci. 2010;352:163–70.
18. Bourg IC, Steefel CI. Molecular dynamics simulations of water structure and diffusion in silica nanopores. J Phys Chem C. 2012;116:11556–64.
19. Kagan M, Lockwood GK, Garofalini SH. Reactive simulations of the activation barrier to dissolution of amorphous silica in water. Phys Chem Chem Phys. 2014;16(20):9294–301.
20. Lockwood GK, Garofalini SH. Proton dynamics at the water-silica interface via dissociative molecular dynamics. J Phys Chem C. 2014;118:29750–9.
21. Leung K, Nielsen IMB, Criscenti LJ. Elucidating the bimodal acid-base behavior of the water-silica interface from first principles. J Am Chem Soc. 2009;131:18358–65.
22. Musso F, Mignon P, Ugliengo P, Sodupe M. Cooperative effects at water-crystalline silica interfaces strengthen surface silanol hydrogen bonding. An ab initio molecular dynamics study. Phys Chem Chem Phys. 2012;14(30):10507–14.
23. Du J, Rimza JM. Atomistic computer simulations of water interactions and dissolution of inorganic glasses. NPJ Mat Deg. 2017;16:1–12.
24. Rimza JM, Yeon J, van Duin AC, Du J. Water interactions with nanoporous silica: comparison of ReaxFF and ab initio based molecular dynamics simulations. J Phys Chem C. 2016;120:24803–16.
25. Tomozawa M, Hepburn RW. Surface structural relaxation of silica glass: a possible mechanism of mechanical fatigue. J Non-Cryst Solids. 2004;346:449–60.
26. Wiederhorn SM, Fett T, Rizzi G, Hoffmann MJ, Guin J-P. Water penetration—its effect on the strength and toughness of silica glass. Met Matl Trans A. 2013;44(3):1164–74.
27. Lezzi PJ, Xiao QR, Tomozawa M, Blanchet TA, Kurkjian CR. Strength increase of silica glass fibers by surface stress relaxation: a new mechanical strengthening method. J Non-Cryst Solids. 2013;379:95–106.
28. Lezzi PJ, Tomozawa M, Hepburn RW. Confirmation of thin surface residual compressive stress in silica glass by FTIR reflection spectroscopy. J Non-Cryst Solids. 2014;390:13–8.
29. Lezzi PJ, Tomozawa M. An overview of the strengthening of glass fibers by surface stress relaxation. Int J Appl Glass Sci. 2015;6:34–44.
30. Shelby JE. Density of vitreous silica. J Non-Cryst Solids. 2004;349:331–6.
31. Bruckner R. The structure-modifying influence of the hydroxyl content of vitreous silicas. Glastech. Ber. 1970;43:8–12.
32. Wiederhorn SM, Yi F, LaVan D, Richter LJ, Fett T, Hoffmann MJ. Volume expansion caused by water penetration into silica glass. J Am Ceram Soc. 2015;98:78–87.

33. Tomozawa M, Aaldenberg EM. The role of water in surface stress relaxation of glass. Phys Chem Glasses: Eur J Glass Sci Technol B. 2017;58:154–64.
34. Wiederhorn SM, Fett T, Rizzi G, Fünfschilling S, Hoffmann MJ, Guin J-P. Effect of water penetration on the strength and toughness of silica glass. J Am Ceram Soc. 2011;94:s196–s203.
35. Fett T, Schell KG, Hoffmann MJ, Wiederhorn SM. Effect of damage by hydroxyl generation on strength of silica fibers. J Am Ceram Soc. 2018;101:2724–6.
36. Tomozawa M, Kim D-L, Agarwal A, Davis KM. Water diffusion and surface strutural relaxation in silica glasses. J Non-Cryst Solids. 2001;288:73–80.
37. Geisinger KL, Gibbs GV, Navrotsky A. A molecular orbital study of bond length and angle variations in frameowork structures. Phys Chem Miner. 1985;11:266–83.
38. Vanheusden K, Korambath PP, Kurtz HA, Karna SP, Fleetwood DM, Shedd WM, et al. The effect of near-interface network strain on proton trapping in SiO_2. IEEE Trans Nucl Sci. 1999;46(6): 1562–7.
39. Lezzi PJ, Evke EE, Aaldenberg EM, Tomozawa M. Surface crystallization and water diffusion of silica glass fibers: causes of mechanical strength degradation. J Am Ceram Soc. 2015;98:2411–21.
40. Mahadevan TS, Garofalini SH. Dissociative water potential for molecular dynamics simulations. J Phys Chem B. 2007;111:8919–27.
41. Soper AK. The radial distribution functions of water and ice from 220 to 673K and at pressures up to 400 MPa. Chem Phys. 2000;258:121–37.
42. Duval Y, Mielczarski JA, Pokrovsky OS, Mielczarske E, Ehrhardt JJ. Evidence of the existence of three types of species at the quartz-aqueous solution interface at pH 0–10: XPS surface group quantification and surface complexation modeling. J Phys Chem B. 2002;106:2937–45.
43. Sato R, Ohkuma S, Shibuta Y, Shimojo F, Yamaguchi S. Proton migration on hydrated surface of cubic ZrO_2: ab initio molecular dynamics simulation. J Phys Chem C. 2015;119:28925–33.
44. Lockwood GK, Garofalini SH. Lifetimes of excess protons in water using a dissociative water potential. J Phys Chem B. 2013;117:4089–97.
45. Lentz J, Garofalini SH. Role of the hydrogen bond lifetimes and rotations at the water/amorphous silica interface on proton transport. Phys Chem Chem Phys. 2019;21:12265–78.
46. Marx D. Proton transfer 200 years after von Grotthuss: insights from ab initio simulations. Chem Phys Chem. 2006;7:1848–70.
47. Lentz J, Garofalini SH. Structural aspects of the topological model of the hydrogen bond in water on auto-dissociation via proton transfer. Phys Chem Chem Phys. 2018;20(24):16414–27.
48. Nakahara M, Matubayasi N, Wakai C, Tsujino Y. Structure and dynamics of water: from ambient to supercritical. J Mol Liq. 2001;90:75–83.
49. Rycroft CH. Voro++: a three-dimensional Voronoi cell library in C++. Chaos. 2009;19:041111.
50. Barber CB, Dobkin DP, Huhdanpaa HT. The Quickhull algorithm for convex hulls. ACM Trans Math Software. 1996;22:469–83.
51. Nienhuys HK, van Santen RA, Bakker HJ. Orientational relaxation of liquid water molecules as an activated process. J Chem Phys. 2000;112(19):8487–94.
52. Woutersen S, Emmerichs U, Bakker HJ. Femtosecond mid-IR pump-probe spectroscopy of liquid water: evidence for a two-component structure. Science. 1997;278:658–60.
53. Woutersen S, Bakker HJ. Ultrafast vibrational and structural dynamics of the protons in liquid water. Phys Rev Lett. 2006;96:138305.
54. Laage D, Stirnemann G, Sterpone F, Hynes JT. Water jump reorientation: from theoretical prediction to experimental observation. Acc Chem Res. 2012;45:53–62.
55. Lawrence CP, Skinner JL. Vibrational spectroscopy of HOD in liquid D2O. III. Spectral diffusion and hydrogen-bonding and rotational dynamics. J Chem Phys. 2003;118:264–72.
56. Sulpizi M, Gaigeot M-P, Sprik M. The silica-water interfaace: how the silanols determine the surface acidity and modulate the water properties. J Chem Theory Comput. 2012;8:1037–47.
57. Gallas J-P, Goupil J-M, Vimont A, Lavalley J-C, Gil B, Gilson J-P, et al. Quantification of water and silanlos species of various silica by coupling IR spectroscopy and in-sity thermogravimetry. Langmuir. 2009;25:5825–34.

How to cite this article: Garofalini SH, Lentz J, Homann M. Molecular mechanism of the expansion of silica glass upon exposure to moisture. *J Am Ceram Soc*. 2020;103:2421–2431. https://doi.org/10.1111/jace.16923